# Efficiency Optimization of LLC Resonant Converters Operating in Wide Input- and/or Output-Voltage Range by On-the-Fly Topology-Morphing Control

Milan M. Jovanović and Brian T. Irving
Power Electronics Laboratory
Delta Products Corporation
5101 Davis Drive, Research Triangle Park, NC, USA

*Abstract*— **This paper presents a control method for efficiency improvement of the LLC resonant converter operating with a wide input-voltage and/or output-voltage range by means of topology morphing, i.e., changing of power converter's topology to that which is the most optimal for given input-voltage and/or output-voltage conditions. The proposed on-the-fly topology-morphing control maintains a tight regulation of the output during the topology transitions, i.e., topology transitions are made without inducing noticeable output-voltage transients. The performance of the proposed topology morphing method is verified experimentally on an 800-W LLC dc/dc converter prototype designed for a 100-V to 400-V input-voltage range.**

## I. Introduction

In many applications power conversion circuits are required to operate with a wide input-voltage and/or output-voltage range. For example, a majority of single-phase ac/dc power supplies used in today's computer and telecom power systems must operate in the universal ac-line range from 90 to 264 $V_{RMS}$ and provide constant- or variable-voltage regulated output(s). Typically, telecom ac/dc power supplies need to provide a regulated output between 42 V to 58 V, whereas power supplies for desktop, networking, and server applications need to deliver a constant-voltage with single or multiple output(s). However, to further improve the energy efficiency, single-output server power supplies with two-level selectable output voltage have been recently introduced. Specifically, this new generation of server power supplies with dynamically adjustable output voltage delivers a 12-V output at full and mid-range loads, whereas at light loads the output voltage is reduced to 6 V to improve the light-load efficiency.

Ac/dc battery chargers are another major class of power converters that operate with a wide input- and output-voltage range. For example, the typical output-voltage range of today's plug-in and battery electric vehicle (EV) on-board chargers is 200-450 V. At the same time, this is also the input-voltage range of on-board dc/dc converters that condition power between the high- and low-voltage batteries.

It is well understood that there is a strong trade-off between the input-voltage and/or output-voltage range and the conversion efficiency [1]-[8]. Power converters operating in a wide input-voltage and/or output-voltage range exhibit a larger efficiency fall-off than their narrow-range counterparts.

Generally, the detrimental effect of wide input and/or output voltage range on the conversion efficiency is more severe in resonant converters than in pulse-width-modulated (PWM) converters. Namely, resonant converters most commonly regulate the output voltage by changing the switching frequency, i.e., by moving the operating point away from the resonant frequency as the input voltage increases and/or output voltage decreases. As a result, they suffer from progressively increased losses as the input- and/or output-voltage range is widened. This is the major reason that resonant dc/dc converters, including the most efficient series-resonant LLC converter topology, are not able to maintain high efficiency across the entire range when input voltage or output-voltage range is wide.

The overall efficiency of converters operating in wide input-voltage and/or output-voltage range can be improved by multi-stage conversion [9]-[12]. Typically in this approach, the regulation task and isolation task are performed in two separate stages, i.e., the first stage is used for regulation, whereas the second stage for isolation. Because the isolation stage is unregulated [9], [11], [12], or semi-regulated [10], i.e., regulated in a very narrow range, its efficiency can be maximized. While this approach has been demonstrated to improve efficiency compared to a single-stage converter, its major drawback is increased number of components which increases the circuit's complexity and cost.

Another approach to deal with very wide input-voltage and/or output-voltage range is to employ topology morphing, i.e., topology change. By changing the topology, the gain of the converter is changed which narrows the effective range that the converter needs to be optimized for, thus, improving efficiency. Several topology-morphing techniques are reported in [13]-[17]. Specifically, in [13], a 3-level half-bridge (HB) LLC converter is modulated as a 2-level converter when the input voltage is in the upper range, whereas for lower-range input voltages it is modulated as a 3-level converter. In [14], the conventional 2-level full-bridge (FB) LLC topology is used in the low-input range, whereas it is changed to the half-bridge (HB) topology when operating in the upper-voltage range. The idea in [14] is further expanded in [15]-[17] by employing two transformers. The major deficiency of the on-the-fly topology-morphing approaches described in [13] and [14] is that the topology transitions are made abruptly so that the output exhibits severe overshoots and undershoots during the transitions. In the approaches in [15]-[17] topology transitions are made by briefly stopping and then soft-restarting the circuit, i.e., by interrupting the power flow, which also results in large output-voltage transients that may be reduced by significantly increasing the output filter capacitance. Both of these transition methods are not desirable in applications that require tight regulation of the output voltage at all times.

978-1-4799-6735-3/15/$31.00 ©2015 IEEE

In this paper, a method of on-the-fly topology morphing of the LLC resonant converter operating with a wide input-voltage and/or output-voltage range that does not exhibit significant voltage transients and does not require increased energy storage components is described. In this approach, the LLC topology is gradually changed between the full bridge (FB) and half bridge (HB) so that a tight output control and uninterrupted power flow are maintained during the transitions. The performance of the proposed topology morphing method is verified on a 48-V, 800-W LLC dc/dc converter designed for a 100-V to 400-V input-voltage range.

## II. Design Trade-Offs of LLC Converter

To facilitate the explanation of LLC converter's design trade-offs in applications with wide input and/or output voltage range, Figs. 1(a), (b), and (c) shows the full-bridge (FB) LLC converter, its fundamental-frequency equivalent circuit, and the dc voltage-conversion ratio, respectively [18], [19]. The FB LLC converter in Fig. 1(a) utilizes magnetizing inductance $L_M$ as a part of the resonant-tank circuit that also includes $L_R$-$C_R$ series-resonant branch. It should be noted that the LLC converter can also be implemented by employing a discrete inductor in parallel to the primary winding instead of using the magnetizing inductance of the transformer.

Generally, the LLC converters employ variable switching-frequency control to regulate the output against input-voltage and load-current changes. This frequency control is implemented with approximately 50% duty cycle of all switches and a small dead time between the commutations of the complementary same-leg switches to achieve ZVS. A wider input-voltage and/or load-current range requires a wider switching-frequency range. Generally, a wide switching frequency range is not desirable because it has a detrimental effect on the performance of the converter. For a given input-voltage and load-current range, the frequency range is dependent on the value of transformer's magnetizing inductance $L_M$. In series-resonant LLC converters, magnetizing inductance $L_M$ is essential in enabling the converter operation at very light and no load by providing a resonant-current path when the load is small or zero. By decreasing magnetizing inductance $L_M$, i.e., by increasing the magnetizing current relative to the primary-referred load current flowing through resistor $n^2R_{ac}$, the frequency range is reduced since with a reduced magnetizing inductance the converter starts behaving more as a parallel resonant converter. However, since the magnetizing current does not flow through the load, as it can be seen from Fig. 1(b), it represents a circulating current which unnecessarily generates conduction loss in the primary switches and the transformer. Therefore, because of a strong tradeoff between the frequency range and primary-side circulating current loss, a proper selection of the magnetizing inductance value is of the utmost importance for optimizing the efficiency of the LLC converter. Typically, for given values of series resonant circuit components $L_R$ and $C_R$ that determine the series resonant frequency $f_S = 1/\sqrt{L_R C_R}$ in Fig. 1(c), the optimal performance is obtained by selecting the magnetizing inductance so that the ratio $L_M/L_R$ is maximized.

As illustrated in the dc-conversion ratio characteristics in Fig. 1(c), in the ZVS operating range that occurs on the negative slopes of the shown constant-Q characteristics (i.e., to the right of their peaks), the switching loss increases as the frequency increases, whereas the circulating current increases as the frequency decreases. This dependence of the circulating current on the frequency is caused by a reduction of magnetizing-inductance reactance $X_{LM}$ with decreasing frequency which causes a larger portion of the resonant current to flow through the magnetizing inductance, as can be seen in Fig. 1(c). The circulating current also increases as the Q-factor for a given operating conditions, i.e., given input voltage $V_{IN}$, output voltage $V_O$, and load current $I_O$, is selected lower. Namely, as can be seen from Fig. 1(c), a lower Q-factor-characteristic exhibits a higher gain $M = nV_O/V_{IN}$ so that required turns ratio $n = N_P/N_S$ for the characteristic with lower Q is also increased. Since according to Fig. 1(b), the current through the primary-referred load is given by $i_{Rac} = (nV_O)/(n^2R_{AC}) = V_O/(nR_{AC})$, the increased value of turns ratio n decreases current $I_{Rac}$ making the magnetizing circulating current a larger portion of the resonant current. As illustrated in Fig. 1(c), the optimal balance between the circulating-current and switching loss occurs around the series resonant frequency $f_S$, where LLC converters exhibit the maximum efficiency. In fact, the LLC converter exhibits an unmatched efficiency when implemented as a dc/dc transformer, i.e., when it operates without a regulation loop at a constant frequency close to the series-resonant frequency of the resonant tank [12].

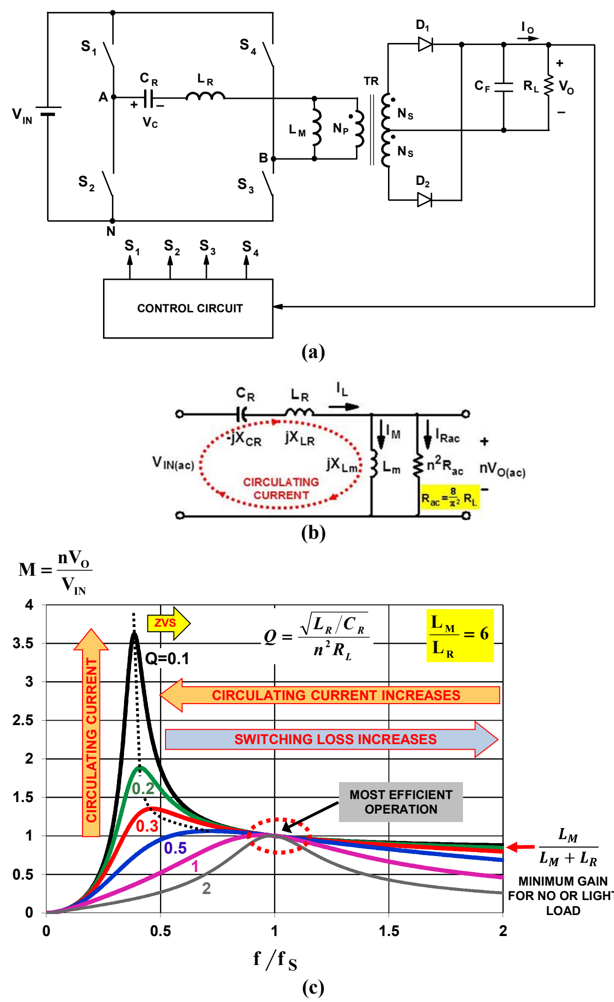


Figure 1. Full-bridge series-resonant LLC converter: (a) circuit diagram; (b) fundamental-frequency equivalent circuit; (c) dc voltage-conversion ratio derived assuming fundamental-frequency approximation [18].

To further explain tradeoffs in designing the LLC converter for a wide input- and/or output-voltage range, Fig. 2 shows the dc-voltage conversion of the LLC converter along with minimum and maximum gain lines that correspond to a 1.5:1 range. Minimum gain $M_{MIN} = nV_{O(MIN)}/V_{IN(MAX)}$ occurs at the minimum output and maximum input voltage, whereas maximum gain $M_{MAX} = n\,V_{O(MAX)}/V_{IN(MIN)}$ occurs at the maximum output voltage and minimum input voltage. As shown in Fig. 2, to maximize efficiency, minimum-gain line $M_{MIN} = 1$ is selected so that at the minimum output- and maximum input-voltage, the converter operates at series-resonant frequency $f_S$. With this selection of $M_{MIN}$, the primary switches operate with ZVS while the secondary-side rectifiers (or synchronous rectifiers) operate with zero-current switching (ZCS). Minimum gain $M_{MIN}$ could also be selected to be less than unity, in which case the secondary-side rectifiers exhibit "hard" switching. In fact, for many designers, based on their personal experience, selecting $M_{MIN}$ slightly below unity, i.e., operating above the resonant frequency, is the preferred choice since this operation is slightly more efficient and does not suffer from a periodic low frequency ripple/noise likely caused by the resonance between the resonant inductor and reflected junction capacitance of the rectifiers seen in the operation below the resonant frequency. However, it should be noted that the lowest value for $M_{MIN}$ is limited to $L_M/(L_M + L_S)$ ratio which represents the minimum gain of the LLC converter at no (light) load. For the characteristics shown in Fig. 2 which are given for $L_M/L_S = 6$, this ratio is 0.86. With the selection of $M_{MIN} = 1$, the maximum gain of the converter operating in the gain range 1.5:1 is $M_{MAX} = 1.5$. To minimize the circulating-current loss at $M_{MAX} = 1.5$, the converter at full load should be designed to operate with a maximum Q-factor which, according to Fig. 2, is $Q = 0.25$. With such a selection of Q-factor, the minimum frequency that occurs at full load and $M_{MAX} = 1.5$ is approximately one-half of resonant frequency $f_S$. Because of the operation significantly below the resonant frequency, the operation at the maximum output and minimum input voltage i.e., at $M_{MAX}$, is less efficient compared to that at the minimum output and maximum input voltage, i.e., at $M_{MIN}$, due to increased circulating-current-caused conduction losses. Nevertheless, for the 1.5:1 range the efficiency fall-off is not very dramatic so that the converter still exhibits satisfactory performance.

Figure 3 shows the $M_{MIN}$ and $M_{MAX}$ gain lines when the range is extended to 3:1. Since the choice of minimum gain $M_{MIN}$ is limited to values around the unity gain, the maximum gain is $M_{MAX} = 3$ if the converter is designed with $M_{MIN} = 1$, as shown in Fig. 3. To minimize circulating-current losses at maximum gain $M_{MAX} = 3$, the converter should be designed with a maximum full-load Q-factor, which according to Fig. 3 is $Q = 0.12$. As it can also be seen from Fig. 3, for $Q = 0.12$, the minimum switching frequency at $M_{MAX}$ is approximately 0.4 of the resonant frequency $f_S$. Because of a lower minimum frequency and a significantly lower Q-factor, operation at the maximum output and minimum input voltage i.e., at $M_{MAX}$, of the wide-range (3:1) converter has significantly lower efficiency compared to that of its narrow-range (1.5:1) counterpart due to increased circulating-current conduction losses. The efficiency performance of both the wide- and narrow-range circuit at the minimum output and maximum input voltage, i.e., at $M_{MIN}$, are similar because both circuits operate close to the resonant frequency.

The efficiency of the LLC converter operating in a very wide input-voltage and/or output voltage range can be improved by recognizing that for the same values of the turns-ratio of the transformer $n = N_P/N_S$ and resonant-tank components $L_R$, $C_R$, and $L_M$, the dc voltage gain of the FB LLC topology is twice as large as that of the half-bridge (HB) LLC topology, as illustrated in Fig. 4. As a result, the FB LLC topology is the optimal choice for a range of operating conditions where the dc voltage gain is high, i.e., where the input voltage is in the low range and/or output voltage is in the high range, whereas the HB LLC topology is more suitable for a range of the input and/or output voltage exhibiting a low dc voltage gain.

Specifically, for the 3:1-range example shown in Fig. 4, the efficiency of the LLC converter can be improved by operating the converter as the FB in the high-gain range, i.e., for gain M between 1.5 and 1, and operating it as the HB for the low-gain range, i.e., for M between 1 and 0.5. Because of the power-stage gain change due to the topology change at $M = 1$, the converter can be designed for a gain range that is only one half of the specified range. As a result of a very much reduced operation range, the efficiency fall-off of the LLC converter with topology changing (morphing) is much less than that of its fixed-topology counterpart. It should be noted that the topology transition does not need to occur exactly at $M = 1$. Depending on a specific design, it may be more optimal to make a transition slightly above or below the unity gain. In fact, the best approach to determine the optimal topology transition gain is to measure the efficiency of the converter in both the FB and HB mode and take the gain where the efficiencies of the FB and HB circuit are equal as the transition gain.

## III. Proposed On-the-Fly Morphing Control

Since the HB LLC topology can be obtained from the FB LLC

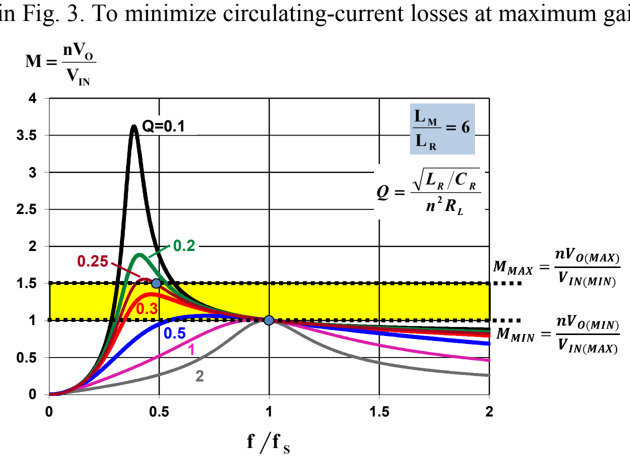


Figure 2. Full-bridge LLC converter operating in 1.5:1 gain range.

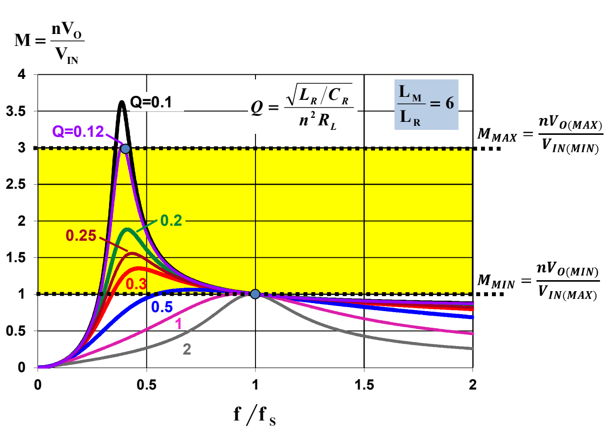


Figure 3. Full-bridge LLC converter operating in 3:1 gain range.

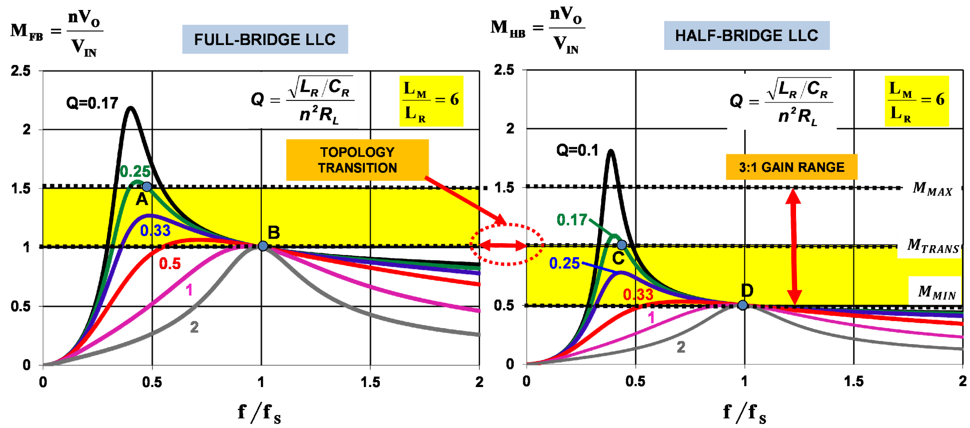


Figure 4. LLC converter operating in 3:1 range with topology morphing. Transition from FB to HB and vice versa occurs at $M_{TRANS}=1$.

topology by not switching one leg of the FB LLC converter, i.e., by permanently keeping one switch in the non-switching leg on and the other switch off, the performance optimization of the LLC converter operating in a very wide input-voltage and/or output voltage range can be obtained with a proper control.

In its simplest form, the on-the-fly controller which provides transitions between the FB and HB LLC topology and vice versa can be implemented so that the modulation of one leg of the bridge is abruptly stopped or restarted [13], [14]. Generally, this approach is not acceptable in applications that require a tight regulation of the output at all times, i.e., in applications that cannot tolerate large output voltage transients. Namely, because in the FB LLC the steady-state average (dc) voltage of resonant capacitor $V_{CR(av)}^{FB} = 0$, whereas in the HB LLC circuit $V_{CR(av)}^{HB} = V_{IN}/2$, an abrupt topology change causes a large initial imbalance of the transformer and resonant inductor volt-seconds, which besides the potential to saturate these components, creates a significant imbalance between the input power and output power. Since the control loop speed (bandwidth) is not fast enough to correct for this abrupt transient power imbalance, the output voltage exhibits unacceptably large output-voltage transients (under and overshoots). Generally, these transients can be reduced by increasing energy storage in the output filter, i.e., by significantly increasing the output capacitance of the LLC converter. However, this approach is not only undesirable because of increased cost, but in high-power density applications it is not practical because it requires increased volume.

To minimize and even eliminate output-voltage transients, as well as possible magnetic component saturations, it is necessary to implement a gradual topology transition. Generally, the topology transition time must be long enough to allow the control loop to maintain a tight regulation of the output during the transition.

The on-the-fly transition control from the FB topology to the HB topology proposed in this paper is illustrated in Fig. 5. During the FB operation, all switches are operated with variable switching frequency and 50% duty ratio. During the transition, switches $S_1$ and $S_2$ continue to operate with variable switching frequency and 50% duty ratio to maintain the output at the desired level, whereas switches $S_3$ and $S_4$ are PWM modulated and frequency modulated so that the duty ratio of $S_3$ is monotonically increased from 50% to 100% and the duty ratio of $S_4$ is reduced from 50% to 0% in a complementary fashion. Since at the end of the transition period switch $S_3$ is permanently on and switch $S_4$ permanently off, the converter continues to operate as the HB converter with variable-frequency control of switches $S_1$ and $S_2$. During the transition from the HB to the FB topology, switches $S_3$ and $S_4$ are modulated in the opposite direction, i.e., the duty ratio of switch $S_3$ is decreased from 100% (continuously on) to 50%, whereas at the same time the duty ratio of $S_4$ is increased from 0% (continuously off) in a complementary fashion. With this topology-transition control, tight output regulation is maintained at all times by frequency regulation of switches $S_1$ and $S_2$.

In the morphing control in Fig. 5, the turn-on instants of switches $S_1$ and $S_3$ are synchronized during the topology transition periods. However, it should be noted that other synchronization methods are possible such as, for example, the turn-on-instant synchronization of switches $S_2$ and $S_4$.

## IV. Design Considerations

Generally, the performance optimization of the LLC converter with topology morphing follows a well-established LLC-converter design procedure [2]-[7], [18]-[21]. Specifically, in the LLC converter with topology morphing, the values of series-resonant tank components $L_R$ and $C_R$, as well as the value of magnetizing inductance $L_M$ and turns ratio n of the transformer are selected so that the performance of the circuit is optimized in the respective narrow gain (input/output voltage) range that it works either as the FB or HB converter.

The only major design difference between the conventional and topology-morphing implementation is the latter one cannot be implemented with magnetically-coupled gate drive of the primary switches in the topology-transition leg $S_3$-$S_4$ because switch $S_3$ must permanently stay on while the converter operates as the HB LLC. As a result, the topology-transition leg must employ a high-

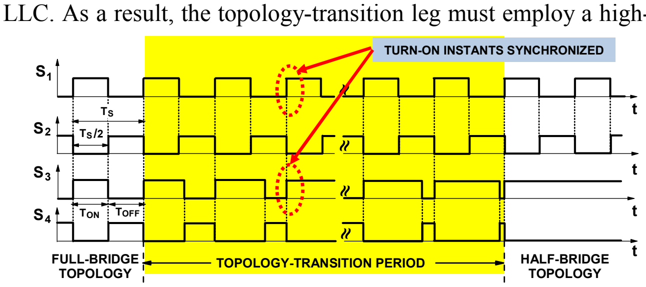


Figure 5. Proposed topology transition control from FB to HB topology. The HB-to-FB transition control is implemented by reverse modulation. Note that during transition period switches $S_3$ and $S_4$ operate with asymmetrical duty cycles and that turn-on instants of switches $S_1$ and $S_3$ are kept synchronized.

side driver, as shown in the experimental circuit in Fig. 8. While the other primary leg does not require a high-side drive because it is continuously modulated, it is a good practice to also use a high-side drive in this leg to maintain primary-side symmetry.

A detailed analysis of the operation of the circuit during topology transitions reveals that switches $S_1$, $S_2$, and $S_3$ maintain ZVS operation at all times. However, transition-leg switch $S_4$ loses ZVS for duty cycles greater than 0.6 because the current through switch $S_3$ becomes negative, i.e., flows through the body diode of switch $S_3$, prior to turn-on of switch $S_4$. As a result, to prevent any noise-related problems that may arise during topology-transition periods because of reverse-recovery current of the body diode of switch $S_3$, it is advisable to employ magnetic beads in the drain and gate of switch $S_3$ to reduce the reverse-recovery current. Although not necessary, it is also a good practice to employ beads in all primary switches to maintain circuit symmetry or, at least in both transition-leg switches as illustrated in Fig. 8.

Since operation with asymmetrical duty cycle introduces magnetizing-current dc-bias $i_{M(av)}$ during transition periods, as shown in Fig. 7, it is necessary to examine the effect of this transient dc-bias on the operation of the transformer. Because an analytical expression for transient magnetizing current dc bias is difficult to derive, simulations of the experimental circuit in Fig.8 were used to quantify and evaluate the dc-bias effect. The first step in this simulation-based analysis was to establish a reference level for this evaluation by finding the maximum steady-state peak value of the magnetizing current when the circuit operates either as the HB or FB converter. By using SIMPLIS simulation software, maximum steady-state peak value of magnetizing current $i_{M(PEAK)}^{MAX}$ was calculated by sweeping the respective input-voltage range, i.e., the 100- 240-V range for the FB topology and the 240-400-V range for the HB topology. As expected, it was found that $i_{M(PEAK)}^{MAX} = 8\,A$ occurs at minimum input voltage of 100 V, i.e., when the circuit operates as FB, because at this operating point the switching frequency is lowest, as can be seen from Fig. 9. Because of symmetrical operation in steady state, the minimum steady-state valley value of magnetizing current is $i_{M(VALLEY)}^{MIN} = -i_{M(PEAK)}^{MAX} = -8\,A$. Next, the average magnetizing current $i_{M(av)}^{TRAN}$, peak magnetizing current $i_{M(PEAK)}^{TRAN}$, and valley magnetizing current $i_{M(VALLEY)}^{TRAN}$ during topology-transition period are calculated as functions of duty cycle $D_{S3}$. Figure 9 shows the calculated $i_{M(av)}^{TRAN}$, $i_{M(PEAK)}^{TRAN}$, and $i_{M(VALLEY)}^{MIN}$ for full-load transition at transition voltage $V_{IN}^{TRAN} = 240\,V$. Also superimposed on the plot in Fig. 9 are the lines for steady-state maximum peak magnetizing current $i_{M(PEAK)}^{MAX} = 8\,A$ and minimum valley magnetizing current $i_{M(VALLEY)}^{MIN} = -8\,A$. As can be seen from Fig.

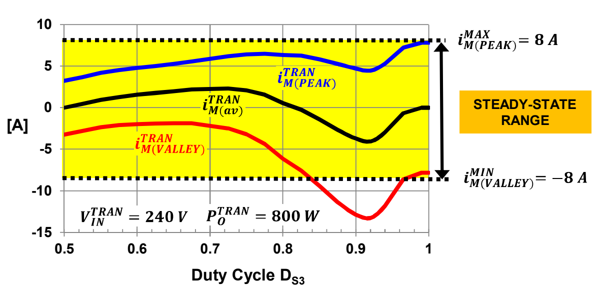


Figure 6. Magnetizing-current transient analysis for experimental circuit in Fig. 9 obtained by SIMPLIS simulation. Shown are peak magnetizing current , $i_{M(PEAK)}^{TRAN}$ minimum (valley) magnetizing current $i_{M(VALLEY)}^{TRAN}$ , and average magnetizing current $i_{M(AV)}^{TRAN}$ as functions of transition duty cycle $D_{S3}$.

6, transient magnetizing-current dc-bias $i_{M(av)}^{TRAN}$ changes from positive to negative as $D_{S3}$ increases and reaches a negative maximum of approximately -4.5 A when $D_{S3}$ is approximately 0.92. During the topology transition period, peak magnetizing current $i_{M(PEAK)}^{TRAN}$ stays within the steady-state range. However, the value of valley magnetizing current $i_{M(VALLEY)}^{TRAN}$ exceeds the maximum steady-state value of -8 A for duty cycles between 0.85 and 0.95. The magnetizing current reaches its absolute minimum value of around -13.5 A for duty cycle $D_{S3}$=0.92. This value is about 70% larger than that in the steady state so this transient increase of the transformer maximum current must be taken into account when designing the transformer.

Finally, the most important design step is to properly determine topology-transition time $T_{TRAN}$. To maintain acceptably small output-voltage transients (overshoots and undershoots), the rate of the duty-ratio change of switches $S_3$ and $S_4$ during the topology transition must be limited to that which allows the control loop to maintain full regulation. The optimal choice of transition time $T_{TRAN}$ and output-loop bandwidth $f_{BW}$ was found to be $T_{TRAN} f_{BW} > 50 - 100$. For example, for the control-loop bandwidth of 1-2 kHz, the transition time can be as fast as 50-100 ms. It should be noted that during the topology-transition periods, small-signal control-to-output transfer function $G_{VC}$ changes with duty cycle $D_{S3}$, as illustrated in Fig. 7 which shows the full-load Bode plots of $G_{VC}$ of the experimental converter in Fig. 9 for different duty cycles $D_{S3}$ that are obtained by SIMPLIS simulations. As can be seen in Fig. 7, both the low-frequency (f<1 kHz) magnitude and transfer function order change during topology transitions. This behavior of $G_{VC}$ is in agreement with the results of small-signal analysis presented in [22]. Namely, since the dc-gain of $G_{VC}$ of the LLC converter is proportional to the slope of the dc-gain characteristic, the $G_{VC}$ dc-gain increases as the circuit makes a transition from the FB to the HB topology because, as illustrated in Fig. 4, at transition gain $M_{TRAN}$, the FB topology operates near the resonant frequency (operating point B) where the slope of the dc characteristic is small, whereas the HB

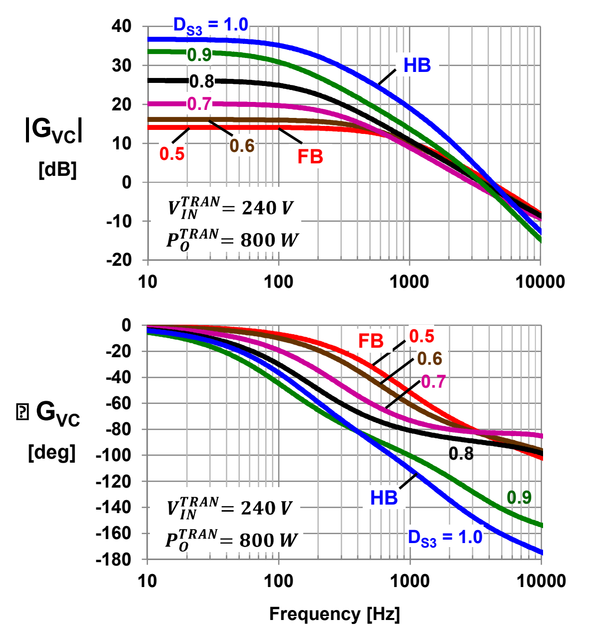


Figure 7. Bode plots of small signal control-to-output transfer function $G_{VC}$ of experimental converter of Fig. 9 as function of duty cycle $D_{S3}$ during topology transitions at full-load. Bode plots were obtained by SIMPLIS simulation software.

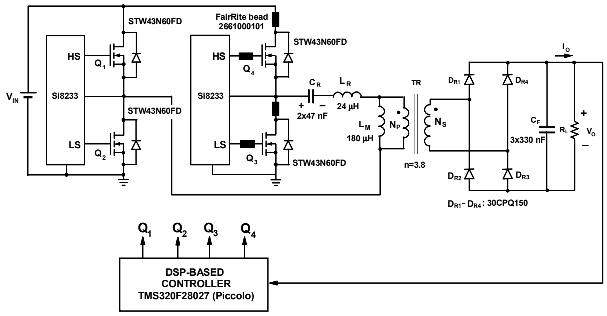

Figure 8. Experimental prototype.

topology operates at a frequency well below the resonant frequency (operating point C) where the slope of dc-characteristic is steeper. In addition, as the switching frequency moves away from the resonant frequency during the topology transition from the FB to the HB topology, the $G_{VC}$ transfer function changes from the first order to the second order [22]. As a result, if a non-adaptive output-voltage control is employed, the transition time needs to be selected based on the worst-case, i.e., the minimum bandwidth. If necessary, an adaptive control that changes compensator parameters as a function of transition duty cycle to maintain optimum bandwidth during the topology transitions can be applied. This adaptive control can be easily and cost-effectively implemented with today's microcontrollers and/or DSPs.

## V. EXPERIMENTAL PERFORMANCE EVALUATION

The performance of the proposed on-the-fly topology morphing control method is verified and evaluated on an 800-W LLC dc/dc converter designed for a 100-V to 400-V input-voltage range and an output voltage of 48-V. The circuit diagram of the power stage of the experimental prototype along with the values of its components are shown in Fig.8. For the selected components, the series-resonant frequency of the circuit is 98 kHz. The control was implemented by TI DSP TMS320F28027 with the control bandwidth at full load and low line of 1 kHz.

Figure 9 shows the measured full-load efficiencies of the experimental converter for both FB and HB topology. Due to the practical switching-frequency limitation of approximately 300 kHz, the FB converter could not regulate the output for input voltages higher than 270 V. It should be noted that the efficiency could have been maximized by employing synchronous rectifiers instead of the diode rectifiers. However, since the main objective of the prototype was to demonstrate and evaluate relative efficiency improvements brought about by the proposed on-the-fly topology morphing, the implementation of the secondary-side is irrelevant with respect to general conclusions about topology morphing performance.

It is interesting to note that the measured peak efficiency of the HB topology of approximately 94.3% is 0.5% higher than the measured peak efficiency of the FB topology of approximately 93.8% although both topologies operate with almost the same switching frequencies and resonant current magnitudes. This difference can be attributed to a lower loss of morphing-leg switches $S_3$ and $S_4$ when the circuit operates as the HB converter. Namely, in the HB topology switch $S_4$ is permanently off so it does not exhibit any losses, whereas switch $S_3$ is permanently on and exhibits only conduction loss due to the resonant current flow through the channel of the switch and, for high peak currents, simultaneous current flow through its body diode. Since in the FB topology switches $S_3$ and $S_4$ are continuously modulated, they exhibit both switching and conduction losses. In addition, since both switches prior to their respective turn on instants carry resonant current through the body diode to achieve ZVS, their conduction loss is further increased compared to the corresponding loss in the HB topology.

As can be seen in Fig. 9, to maximize the efficiency across the entire input-voltage range, the topology transition voltage is selected at the intersection of the FB and HB efficiency curves, i. e., at 240 V. The full-load efficiency in the entire range is determined by that at the minimum input voltage of 100 V, which is approximately 90.5%. If the FB were able to operate in the entire input-voltage range from 100-400 V, i.e., if the controller were able to provide required frequency range, the full-load efficiency at 400-V input would be very much below 90% as illustrated by the extrapolated efficiency line in Fig. 9.

Figure 10 shows the key waveforms during the topology

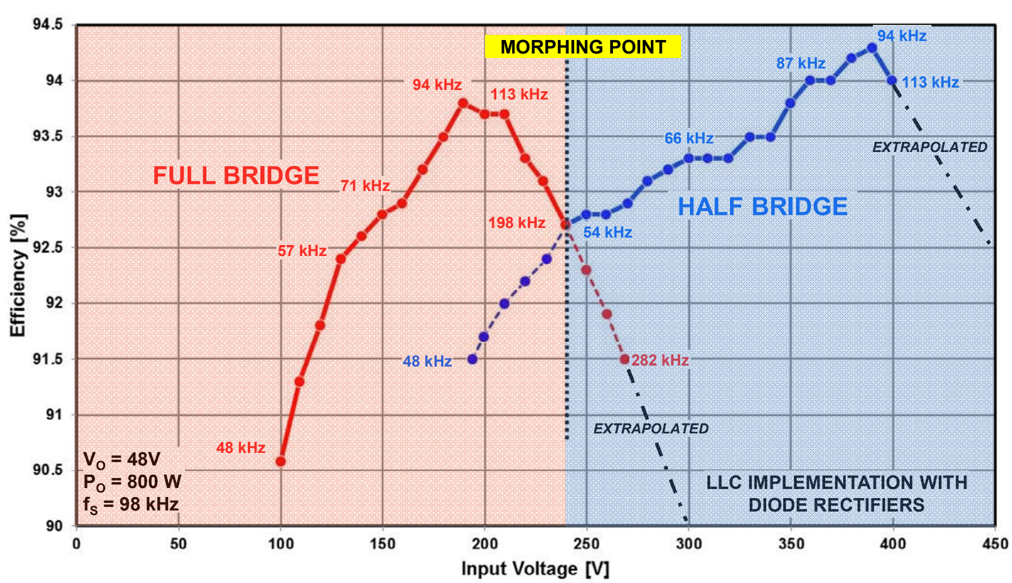


Figure 9. Measured full-load efficiency of experimental converter for both full bridge and half bridge topology. Dashed-dot line shows extrapolated efficiency.

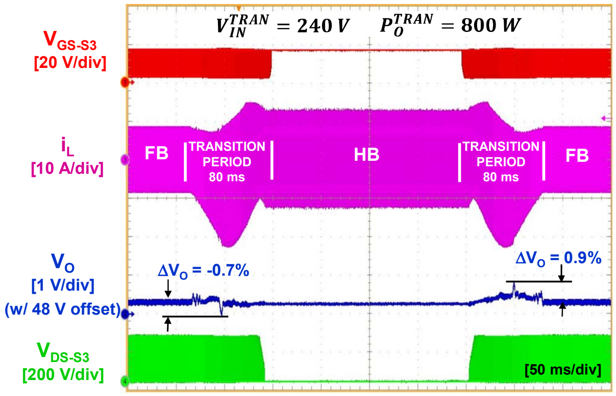


Figure 10. Measured switch $S_3$ gate-to-source voltage $V_{GS\text{-}S3}$, resonant current $i_L$, output voltage $V_O$, and switch $S_3$ drain-to-source voltage $V_{DS\text{-}S3}$ waveforms of experimental circuit for 80-ms topology transitions at $V_{IN}^{TRAN} = 240\ V$ and $P_O^{TRAN} = 800\ W$.

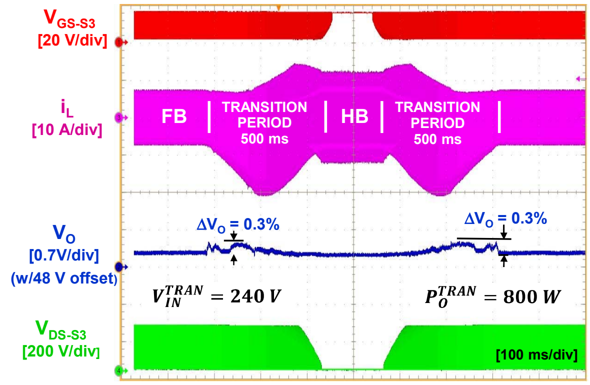


Figure 11. Measured switch $S_3$ gate-to-source voltage $V_{GS\text{-}S3}$, resonant current $i_L$, output voltage $V_O$, and switch $S_3$ drain-to-source voltage $V_{DS\text{-}S3}$ waveforms of experimental circuit for 500-ms topology transitions at $V_{IN}^{TRAN} = 240\ V$ and $P_O^{TRAN} = 800\ W$.

transition at full load. As can be seen during the 80 ms transition periods, the output voltage transients are limited to below 0.9%. Specifically, the maximum positive deviation from the steady-state output voltage (overshoot) is 0.9%, whereas maximum negative deviation (undershoot) is -0.7%. During transitions, the peak of resonant current $i_L$ exceeds its steady-state value by approximately 50%, which is still well within the design margins of inductor $L_R$. For a given control design, the overshoot and undershoot of the output voltage is smaller if the transition time is longer. As illustrated in Fig. 11, for the 500-ms transition time, the maximum transient deviation of the output voltage is only 0.3%.

Figure 12 shows the zoomed in waveforms in Fig. 10 during the transition from the FB to the HB topology. As can be seen, the shown $V_{GS\text{-}S3}$, $i_L$, and $V_{DS\text{-}S3}$ waveforms for transition duty cycles $D_{S3} = 0.55$ and $D_{S3} = 0.75$ do not exhibit any ringing or irregularities. In addition, the output voltage stays in regulation without any noticeable transients.

Finally, Fig. 13 shows the key waveforms during the output voltage transitions between 48-V and 24-V level. These transitions, with a transition time of 300 ms, are performed at constant input voltage $V_{IN} = 200$ V and constant load current $I_O = 16.6$ A by changing (ramping up and down) the output reference voltage during the topology transition periods. Because of the constant-current load, the output power at $V_O = 24\ V$ is one half of that at $V_O = 48\ V$, i.e., when the circuit operates as the FB for $V_O = 48\ V$, it delivers 800 W, whereas it delivers only 400 W when it operates as the HB for $V_O = 24\ V$. As can be seen from

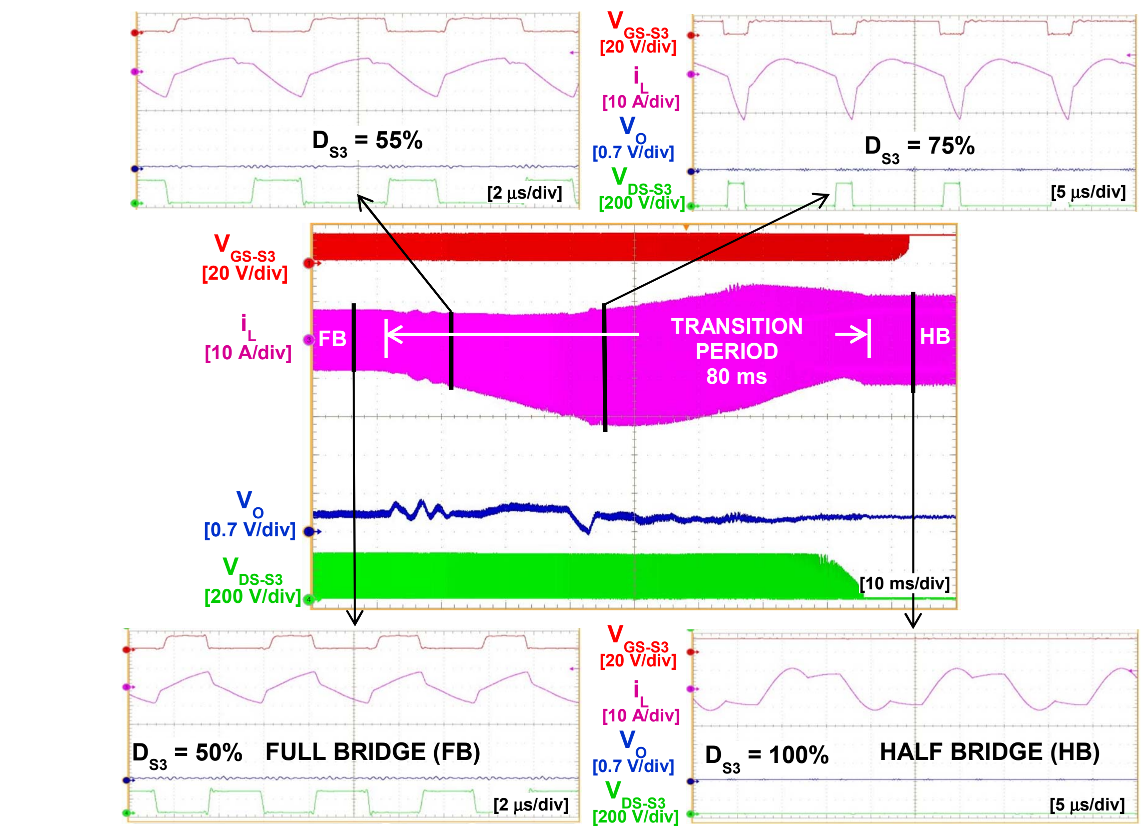


Figure 12. Zoomed-in waveforms of Fig. 13 for FB-to-HB transition for duty cycle $D_{S3}$=50, 55, 75, and 100%.

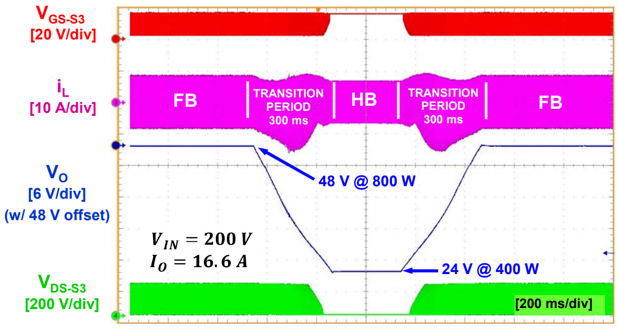


Figure 13. Measured waveforms for output voltage transitions between 48-V and 24-V level at $V_{IN} = 240\ V$ and constant load current $I_O = 16.6\ A$.

Fig. 13, the output voltage for both ramp down and up transitions changes monotonically without any overshoots and/or undershoots.

## VI. Summary

In this paper, a control method for on-the-fly topology change, i.e., topology morphing, employed to optimize efficiency of the LLC resonant converter operating with a wide input-voltage and/or output-voltage range is described. In the proposed approach, the LLC topology is gradually changed between the full bridge (FB) and half bridge (HB) so that a tight output control and uninterrupted power flow are maintained during the transitions. As a result, the output voltage does not exhibit any significant transients during the topology-transition periods.

By changing of power converter's topology to that which is the most optimal for given input-voltage and/or output-voltage conditions, converter's efficiency can be improved. The full-bridge topology is employed when the ratio of the input voltage to the output voltage is in the high range, i.e., when the input voltage is low and/or the output voltage is high, whereas the topology is changed to the half bridge when the input to the output voltage ratio in the low range, i.e., when the input voltage is high and/or the output voltage is low.

The transition between the two topologies is implemented by pulse-width-modulation of the two switches in one of the bridge legs. Specifically, when transitioning from the full-bridge to the half-bridge topology, the duty ratio of one switch is increased from 50% to 100%, while simultaneously the duty ratio of the other switch is reduced from 50% to 0% so that after the transition, one switch is continuously kept on while the other is continuously turned off. The transition from the half-bridge to the full-bridge topology is accomplished by commencing the modulation of the non-switching leg and changing the duty ratios of the switches until they both operate with 50% duty ratio.

The performance of the proposed on-the-fly topology-morphing control is experimentally verified on a 48-V, 800-W, LLC dc/dc converter prototype designed for a 100-V to 400-V input-voltage range. The measured results show that the output voltage stays tightly regulated during topology transitions, exhibiting transients that are below 1% for a transition time as short as 80 ms.

## References

[1] F. Canales, P. Barbosa, and F. C. Lee, "A wide input voltage and load output variations fixed-frequency ZVS DC/DC LLC resonant converter for high-power applications," in *Proc. IEEE Appl. Power Electron. Conf. (APEC)*, 2002, pp. 2306-2313.

[2] Y. Liu, "High efficiency optimization of LLC resonant converter for wide load range," M.S. thesis, Virginia Polytechnic Inst. & State Univ., Blacksburg, VA, 2007.

[3] Y. Fang, D. Xu, Y. Zhang, F. Gao, and L. Zhu, "Design of high power density LLC resonant converter with extra wide input range," in *Proc. IEEE Appl. Power Electron. Conf. (APEC)*, 2007, pp. 976-981.

[4] R. Beiranvand, B. Rashidian, M. R. Zolghadri, and S. M. H. Alavi, "Using LLC resonant converter for designing wide-range voltage source," *IEEE Trans. Industrial Electron.*, vol. 58, no. 5, pp. 1746-1756, May 2011.

[5] X. Fang, H. Hu, Z. J. Shen, and I. Batarseh, "Operation mode analysis and peak gain approximation of the LLC resonant converter," *IEEE Trans. Power Electron.*, vol. 27, no. 4, pp. 1985-1995, Apr. 2012.

[6] D. S. Gautam, F. Musavi, M. Edington, W. Eberle, and W. G. Dunford, "An automotive onboard 3.3-kW battery charger for PHEV application," *IEEE Trans. Vehicular Technol.*, vol. 61, no. 8, pp. 3466-3474, Oct. 2012.

[7] F. Musavi, M. Craciun, D. S. Gautam, W. Eberle, and W. G. Dunford, "An LLC resonant dc-dc converter for wide output voltage range battery charging applications," *IEEE Trans. Power Electron.*, vol. 28, no. 12, pp. 5437-5445, Dec. 2013.

[8] T. LaBella, W. Yu, J.-S. Lai, M. Senesky, and D. Anderson, "A bidirectional-switch-based wide-input range high-efficiency isolated resonant converter for photovoltaic applications," *IEEE Trans. Power Electron.*, vol. 29, no. 7, pp. 3473-3484, July 2014.

[9] J. Drobnik, "Is cascade connection of power converters inefficient?," in *Proc. Power Conversion & Intelligent Motion Conf. (PCIM)*, 1993, pp. 34-43.

[10] Y. Jang and M. M. Jovanović, "Fully soft-switched three-stage ac-dc converter," *IEEE Trans. Power Electron.*, vol. 23, no. 6, pp. 2884-2892, Nov. 2008.

[11] M. F. Schlecht, "A two-stage approach to highly efficient, super-wide input voltage range DC-DC converters," *Technical White Paper*, Synqor Inc., MA [Online]. Available: http://www.synqor.com/documents/whitepapers/wp_Two-Stage_Approach.pdf.

[12] M. Salato, "The sine amplitude converter topology provides superior efficiency and power density in intermediate us architecture applications," *Technical White Paper*, Vicor Corp., MA [Online] Available: http://www.vicorpower.com/documents/whitepapers/wp_sac.pdf

[13] A. Coccia, F. Canales, P. Barbosa, and S. Ponnaluri, "Wide input voltage compensation in Dc/DC resonant architectures for on-board traction power supplies," in *Proc. 12th European Conf. on Power Electron. and Appls., 2007,* pp. 1-10.

[14] Z. Liang, R. Guo, G. Wang, and A. Huang, "A new wide input range high efficiency photovoltaic inverter," in *Proc. IEEE Energy Conversion Congress and Expo(ECCE)*, 2010, pp. 2937-2943.

[15] Z. Liang, R. Guo, J. Li, and A.Q. Huang, "A high-efficiency PV module-integrated DC/DC converter for PV energy harvest in FREEDM systems," *IEEE Trans. Power Electron.*, vol. 26, no. 3, pp. 897-909, Mar. 2011.

[16] H. Hu, X. Fang, Q. Zhang, Z. J. Shen, and I. Batarseh, "Optimal design considerations for a modified LLC converter with wide input voltage range capability suitable for PV applications," in *Proc. IEEE Energy Conversion Congress and Expo (ECCE)*, 2011, pp. 3096-3103.

[17] H. Hu, X. Fang, F. Chen, Z. J. Shen, and I. Batarseh, "A modified high-efficiency LLC converter with two transformers for wide input-voltage range applications," *IEEE Trans. Power Electron.*, vol. 28, no. 4, pp. 1946-1960, Apr. 2013.

[18] T. Duerbaum, "First harmonic approximation including design constraints," in *Proc. IEEE Int'l Telecommunications Energy Conf.* (INTELEC), 1998, pp. 321-328.

[19] S. D. Simone, C. Adragna, C. Spini and G. Gattavari, "Design-oriented steady state analysis of LLC resonant converters based on FHA," in *Proc. IEEE Int'l Symp. Power Electronics, Electric Drives, Automation & Motion (SPEEDAM),* 2006, pp.16-23.

[20] B. Yang, F. C. Lee, A. J. Zhang, and G. Huang, "LLC resonant converter for front end DC/DC conversion," in *Proc. IEEE Appl. Power Electron. Conf. (APEC)*, 2002, pp. 1108-1112.

[21] B. Lu, W. Liu, Y. Liang, F. C. Lee, and J. D. van Wyk, "Optimal design methodology for LLC resonant converter," in *Proc. IEEE Appl. Power Electron. Conf. (APEC)*, 2006, pp. 533-538.

[22] B. Yang, "Topology investigation for front end DC/DC power conversion for distributed power system," Ph.D. dissertation, Virginia Polytechnic Inst. & State Univ., Blacksburg, VA, 2003.